An insulin-like peptide regulates egg maturation and metabolism in the mosquito *Aedes aegypti*

Mark R. Brown*†, Kevin D. Clark*, Monika Gulia*, Zhangwu Zhao*‡, Stephen F. Garczynski*§, Joe W. Crim¶, Richard J. Suderman*, and Michael R. Strand*†

Departments of *Entomology and ¶Cellular Biology, University of Georgia, Athens, GA 30602

Edited by David L. Denlinger, Ohio State University, Columbus, OH, and approved March 6, 2008 (received for review January 16, 2008)

Ingestion of vertebrate blood is essential for egg maturation and transmission of disease-causing parasites by female mosquitoes. Prior studies with the yellow fever mosquito, *Aedes aegypti*, indicated blood feeding stimulates egg production by triggering the release of hormones from medial neurosecretory cells in the mosquito brain. The ability of bovine insulin to stimulate a similar response further suggested this trigger is an endogenous insulin-like peptide (ILP). *A. aegypti* encodes eight predicted ILPs. Here, we report that synthetic ILP3 dose-dependently stimulated yolk uptake by oocytes and ecdysteroid production by the ovaries at lower concentrations than bovine insulin. ILP3 also exhibited metabolic activity by elevating carbohydrate and lipid storage. Binding studies using ovary membranes indicated that ILP3 had an IC_{50} value of 5.9 nM that was poorly competed by bovine insulin. Autoradiography and immunoblotting studies suggested that ILP3 binds the mosquito insulin receptor (MIR), whereas loss-of-function experiments showed that ILP3 activity requires MIR expression. Overall, our results identify ILP3 as a critical regulator of egg production by *A. aegypti*.

endocrinology | insect | reproduction | vector

Vertebrates and invertebrates produce a diversity of insulin-like peptide (ILP) superfamily members distinguished by a shared structural motif (1–3). Most ILPs are expressed as prepropeptides that consist of four major domains (Pre, B, C, and A). Humans and other mammals produce up to 10 ILPs that are further subdivided into insulin, insulin-like growth factors (IGFs), and relaxins on the basis of primary structure, processing, and receptor binding preferences. Insulin is the only ILP that binds with high affinity to a homodimer receptor tyrosine kinase (RTK) (≈500 kDa) called the insulin receptor (IR) and stimulates a signaling pathway that includes phosphoinositide 3-kinase (PI3K) and serine/threonine kinase (AKT). IGFs preferentially bind a related RTK [IGF receptor (IGFR)] and activate the MAPK pathway, and relaxins bind G protein-coupled receptors (GPCRs) (4–6). Together, these hormones mediate a diversity of processes with insulin primarily regulating metabolism, IGFs regulating cell proliferation and survival, and relaxins mediating vasodilation.

Insects and other invertebrates also encode multiple ILPs, but their primary structure differs from mammalian family members (7, 8). Homology searches also suggest differences exist between invertebrates and vertebrates in the repertoire of receptors and downstream signaling pathway components that interact with ILPs. For example, *Drosophila*, *Caenorhabditis elegans*, and the mosquitoes *Aedes aegypti* and *Anopheles gambiae* encode only one RTK related to vertebrate IRs and IGFRs. Genetic studies suggest multiple ILPs may activate this receptor and stimulate signal transduction through both PI3K/AKT and MAPK pathways (7, 9). Yet no invertebrate ILP has actually been shown to bind with high affinity to an invertebrate IR homolog and stimulate a specific dose-responsive biological function.

A key feature of mosquitoes that transmit disease-causing pathogens is that they must blood-feed on hosts to produce eggs (10). In *A. aegypti*, blood ingestion triggers the release of neuropeptides from the brain medial neurosecretory cells (MNCs) that stimulate the production of ecdysteroid hormones by the ovaries (10–13). Ecdysteroids then induce the fat body to secrete yolk proteins, derived from nutrients acquired in the blood meal, which are packaged into eggs. Prior studies indicated that mosquito brain extracts and bovine insulin each stimulate ecdysteroid production by the ovaries (14). *A. aegypti* also encodes eight predicted ILP family members of which three (ILP1, ILP3 and ILP8) are specifically expressed in brains of adult females (15). Combined with the finding that ovaries express IR [mosquito IR (MIR)] and AKT (16–18) homologs, these results suggest an endogenous ILP of brain origin stimulates egg maturation by activating the insulin signaling pathway in the ovaries. Here, we report the identification of ILP3 as a regulator of these processes.

Results

***A. aegypti* and Mammalian ILPs Exhibit Structural Differences.** We first assessed whether particular *A. aegypti* ILPs were structurally more similar to mammalian insulin than others. Mammals process the intervening C domain of pro-insulin to produce a mature, secreted peptide comprised of separate B and A chains linked by two interchain disulfide bridges plus a third intrachain bridge in the A chain (Fig. 1*A*). IGFs form the same disulfide bridges but remain single peptides at maturity because their C chain is not cleaved, whereas relaxins are processed like insulin but exhibit differences in primary structure that include the presence of basic lysine and/or arginine residues flanking the first cysteine of the B chain (5, 19). Each *A. aegypti* ILP exhibits intron/exon organization similar to other insulin superfamily members (15). Each *A. aegypti* ILP propeptide with the possible exception of ILP6 also contains sites flanking the C chain, suggesting insulin/relaxin-like processing (15), whereas cysteine spacing patterns suggested conservation in disulfide bridge formation with mammalian ILPs (Fig. 1).

We next compared the primary structure of the mosquito ILPs to selected mammalian and insect family members because receptor binding preferences and biological activities are known to be affected by specific residues in the A and B chains. Essential residues implicated in insulin binding to the IR include Gly-1, Gln-5, Tyr-19, and Asn-21 on the A chain and Tyr-16, Gly 23, Phe-24, Phe-25, and Tyr-26 (GFFY motif) on the B chain that together form the "classical binding surface" (Fig. 1*A*) (2, 20–22). Other important residues include IleA2 and ValA3, which are likely exposed

Author contributions: M.R.B., K.D.C., and M.R.S. designed research; M.R.B., K.D.C., M.G., Z.Z., S.F.G., J.W.C., R.J.S., and M.R.S. performed research; K.D.C. contributed new reagents/analytic tools; M.R.B., K.D.C., R.J.S., and M.R.S. analyzed data; and M.R.B. and M.R.S. wrote the paper.

The authors declare no conflict of interest.

This article is a PNAS Direct Submission.

Data deposition: The sequences reported in this paper have been deposited in the GenBank database (accession nos. DQ845750–DQ845758).

†To whom correspondence may be addressed. E-mail: mrbrown@uga.edu or mrstrand@uga.edu.

‡Present address: Department of Entomology, College of Agricultural and Biotechnology, China Agricultural University, 2 Yuanmingyuan West Road, Beijing 100094, China.

§Present address: Yakima Agricultural Research Laboratory, U.S. Department of Agriculture–Agricultural Research Service, 5230 Konnowac Pass Road, Wapato, WA 98951.

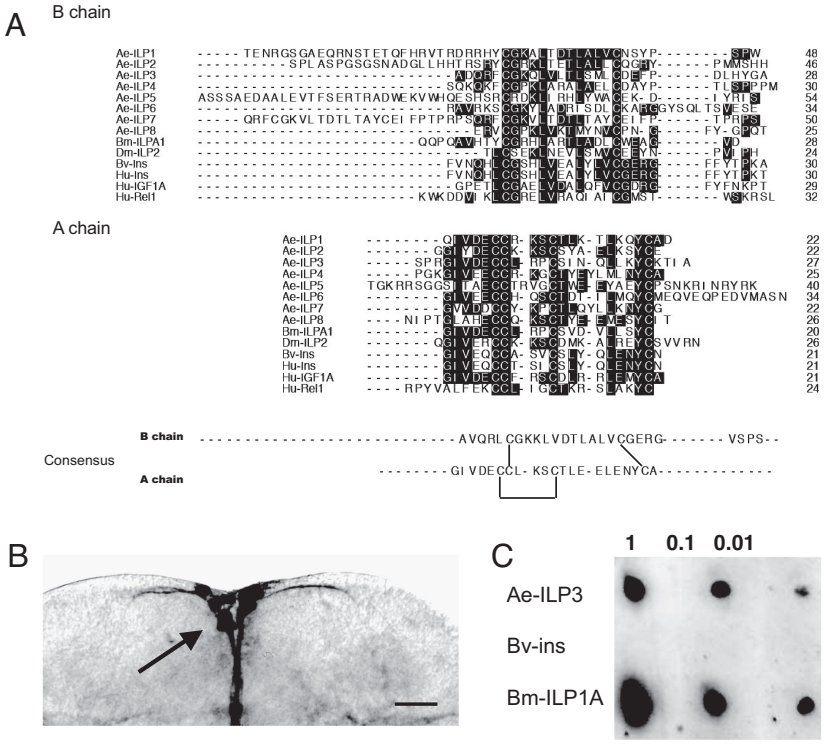

Fig. 1. *A. aegypti* (Ae) ILPs share features with other ILP family members. (*A*) Sequence alignment of the predicted B and A chains for Ae-ILP1–8 with *B. mori* ILPA1 (Bm-ILPA1: Q17192), *Drosophila melanogaster* ILP2 (Dm-ILP2:AAF50204), bovine insulin (Bv-Ins: PO1317), human insulin (Hu-Ins: AAA59172), human IGF factor 1A (Hu-IGF1A:CAA01955), and human relaxin 1 (Hu-Rel1: CAA00599). Residues shared by a majority of family members are shaded in black. The consensus B and A chains are shown below the alignment with the predicted intrachain disulfide bond in the A chain and two interchain disulfide bonds indicated. (*B*) Immunocytochemical whole mount of the *A. aegypti* brain probed with anti-Bm-ILPA1. The arrow indicates strong staining of MNCs and their axons (Scale bar: 50 μm.) (*C*) Immunoblot of serially diluted (1–0.01) ILP3 (3 μg), Bv-Ins (8 μg), and Bm-ILPA1 (1 μg) probed with anti-Bm-ILPA1 (1:4K).

during binding to the IR, and LeuA13, ValB12, and LeuB17 that maintain secondary structure. As previously noted, ILP1, ILP3, and ILP8 are the most likely candidates for regulating egg maturation in *A. aegypti*, because they are exclusively expressed in the brains of adult females, and the brain MNCs are the source of factors that trigger egg maturation after a blood meal (15). Each of these ILPs shared some essential residues with insulin and exhibited overall sequence identities of 43%, 52%, and 38%, respectively, with the bovine insulin A chain and 27%, 29%, and 24% to the B chain. Unlike insulin though, none of the *A. aegypti* ILPs possessed an Asp or related polar residue at the C termini of their A chains or a GFFY motif in their B chains (Fig. 1*A*). Each *A. aegypti* ILP also had one or more basic residues flanking the first Cys of the B chain similar to relaxins (Fig. 1*A*), whereas ILP1, ILP2, ILP5, and ILP7 had N-terminally extended B chains unlike any mammalian ILP. Given these data, we conducted homology modeling studies to assess whether ILP1, ILP3, and ILP8 more closely matched the tertiary structure of human insulin and relaxin2. Analysis of the structures generated by Swiss Model using Anolea, Gromos, and Verify 3D indicated that each ILP favored the insulin fold. ILP8 favored a human insulin and relaxin2 near equally, whereas the large N-terminal extension in the A chain resulted in ILP1 not favoring either template. ILP3 fit insulin better than ILP1 but could not be threaded onto the relaxin2 template despite relatively good sequence alignment. Taken together, these results suggested most *A. aegypti* ILPs are processed like mammalian insulins and relaxins while also revealing that their primary structures were neither fully insulin nor relaxin-like. We therefore selected ILP3 for further study, because of its brain-specific expression and overall greater similarity to mammalian insulins and *Bombyx mori* ILPA1 (see below) than ILP1 and ILP8.

Synthetic ILP3 Is Recognized by Anti-ILPA1. Purifying sufficient ILP3 for functional studies was deemed impractical because of the small size of mosquitoes. Despite the use of recombinant methods two decades ago to produce human insulin (23), we also decided against a molecular strategy to produce ILP3 because of the complexity still required to form a mature peptide. We thus developed a synthetic approach based on methods used for silkmoth ILPs and relaxin (24, 25). After purification, mass spectral analysis confirmed the synthetic peptide corresponded to the predicted structure of mature ILP3. Because prior studies indicated that a monoclonal antibody against *B. mori* ILPA1 specifically labels *A. aegypti* MNCs (11, 15, 26) (Fig. 1*B*), we examined whether this antibody recognized synthetic ILP3. Immunoblotting revealed it bound to ILP3 and ILPA1 but not bovine insulin at any concentration tested (Fig. 1*C*).

ILP3 Stimulates Egg Maturation. Decapitation of *A. aegypti* females by 1 h post blood meal (pbm) inhibits egg maturation because of the loss of stimulatory factors from the brain (13). To assess whether synthetic ILP3 rescued this effect, we used a well established *in vivo* assay. Injection of a single dose of ILP3 over a range of 2 to 125 pmol stimulated yolk uptake by oocytes in $\geq$40% of decapitated mosquitoes. This response was significantly greater than in saline-injected controls where no yolk uptake occurred but was lower than in normal (nondecapitated) blood-fed mosquitoes (Fig. 2*A*). Activity was also hormetic because no yolk uptake occurred in mosquitoes injected with $<$1 pmol or $>$250 pmol of peptide. All primary oocytes in both ovaries contained a similar amount of yolk in females exhibiting a yolk deposition response (Fig. 2*A*). These results implicated ILP3 as a regulator of egg maturation, but yolk deposition is also an indirect measure of activity that depends on sustained ovarian production of ecdysteroid hormones that activate the fat body to secrete yolk proteins. We therefore compared the ability of ILP3 and bovine insulin to induce ecdysteroid synthesis by ovaries from sugar-fed (nonoogenic) mosquitoes in an *in vitro* assay. These experiments indicated that both peptides stimulated a dose-dependent increase in ecdysteroid production from basal levels to $\approx$150 pg per ovary culture (Fig. 2 *B* and *C*). Notably though, a maximal response required only 1 pmol of ILP3 but 100 pmol of bovine insulin.

ILP3 Reduces Hemolymph Sugar Levels and Elevates Carbohydrate and Lipid Stores. Mammalian insulins induce glucose uptake by cells, inhibit glycogen breakdown, and shift lipid metabolism from a catabolic to anabolic state (27). To test whether ILP3 exhibited such

BIOCHEMISTRY

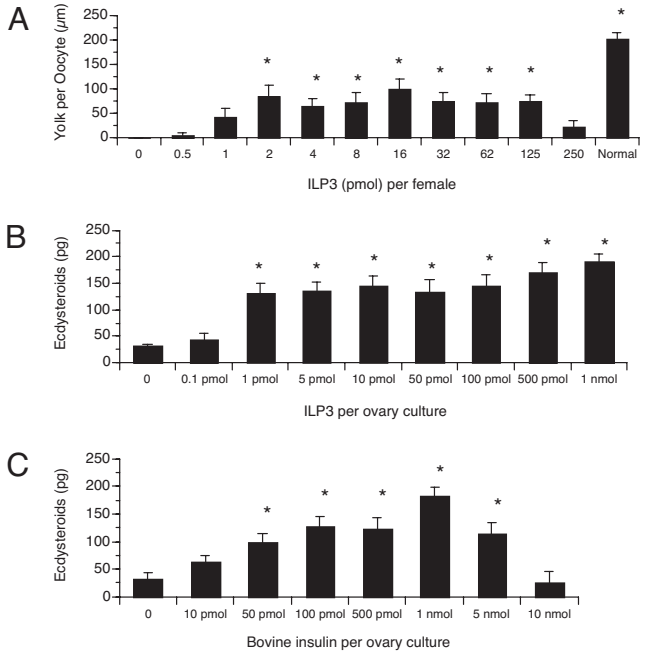

Fig. 2. ILP3 and bovine insulin stimulate yolk uptake or ecdysteroid production by ovaries of female *A. aegypti*. (*A*) Yolk uptake (μm ± SE) by oocytes after injection of ILP3 (0.5–250 pmol per mosquito). Adult females were decapitated within 1 h pbm and injected with ILP3. Females injected with saline served as negative controls, while normal (nondecapitated, saline injected) blood-fed females were positive controls. Asterisks indicate a given treatment differed significantly from the negative control ($F_{11,\ 257} = 12.1$; $P < 0.0001$; followed by Dunnett's multiple-comparison procedure). (*B*) Ecdysteroid production (pg ± SE) by ovaries after incubation with ILP3 (0.1 pmol-1 nmol). Ovaries from sugar-fed females (four pairs) were incubated 6 h with increasing amounts of ILP3 followed by quantification of ecdysteroids. Ovaries incubated without ILP3 served as the negative control. Asterisks indicate a given treatment differed significantly from the negative control ($F_{8,\ 33} = 7.5$; $P < 0.0001$). (*C*) Ecdysteroid production (pg ± SE) by ovaries after incubation with bovine insulin (10 pmol–10 nmol). Ovaries were cultured and ecdysteroids were assayed as in *B*. Asterisks indicate a given treatment differed significantly from the negative control ($F_{7,\ 71} = 10.2$; $P < 0.0001$).

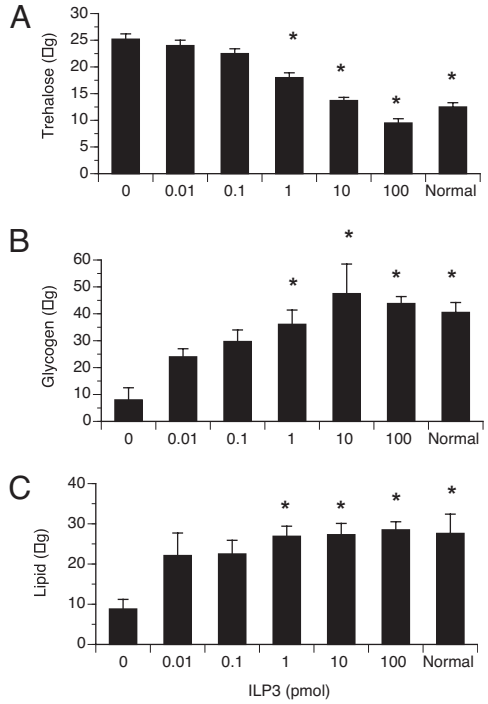

Fig. 3. ILP3 reduces circulating trehalose levels and increases glycogen and lipid stores in female *A. aegypti*. Mosquitoes were decapitated after sugar feeding and injected with ILP3 (0.01–100 pmol) or saline only (negative control). Sugar-fed, normal (nondecapitated) females served as positive controls. Trehalose (*A*), glycogen (*B*), and lipid (*C*) were extracted and assayed from replicate samples of two females. (*A*) Trehalose (μg ± SE) amounts per mosquito 6 h after injection of ILP3. Asterisks indicate a given treatment differed significantly from the negative control ($F_{6,148} = 51.0$; $P < 0.0001$). (*B*) Glycogen (μg ± SE) amounts per mosquito 24 h after injection of ILP3. Asterisks indicate a given treatment differed significantly from the negative control ($F_{6,\ 20} = 2.9$; $P = 0.04$). (*C*) Lipid (μg ± SE) amounts per mosquito 24 h after injection of ILP3. Asterisks indicate a given treatment differed significantly from the negative control ($F_{6\ 20} = 3.2$; $P = 0.03$).

activity, we decapitated sugar-fed females to remove the source of endogenous ILPs. We then injected different doses of ILP3 and measured carbohydrate and lipid levels 6 or 24 h later. After 6 h, ILP3 reduced circulating sugars in the decapitated females to similar levels as controls (Fig. 3*A*) but had no effect on glycogen or lipid levels (data not presented). By 24 h, however, ILP3 elevated glycogen and lipid stores in the decapitated females to the same levels as controls (Fig. 3 *B* and *C*).

ILP3 Binds with High Affinity to Ovary Membranes. Like vertebrate IRs and IGFRs, the MIR proreceptor is processed into an extracellular α-subunit that includes the predicted ligand binding domain and a β-subunit that contains a transmembrane region linked to a characteristic tyrosine kinase domain (16, 17). The mature MIR then forms a 400- to 500-kDa homodimer comprised of two α- and β-subunits that in ovaries localizes primarily to follicle cells (17). Sequence alignments during the current study further indicated the MIR is 37% identical to the human IR overall and 32% identical in the predicted IR ligand binding domain (28). Competitive radio-receptor assays using ovary membranes indicated that ILP3 had an IC_{50} value of 5.9 nM (Fig. 4*A*). Unlabeled ILP3 fully competed binding, whereas unlabeled ILP3 B chain peptide (10 nM–10 μM) and bovine insulin (1 μM–500 μM) were poor competitors. Cross-linking experiments with ovary membranes and 250 pmol of ^{125}I-ILP3 followed by SDS/PAGE and autoradiography detected a single band of >500 kDa (Fig. 4*B*). Intensity of this band was reduced but not eliminated by the addition of cold ILP3 competitor. On companion immunoblots, MIR-specific antibody detected this same single band in cross-linked samples and a single band of ≈500 kDa (the expected size for the MIR) in the noncross-linked sample (Fig. 4*B*).

MIR Expression Is Required for ILP3 Activity. We assessed whether ILP3 activity depended on the MIR by conducting reverse genetic studies. Injection of blood-fed female mosquitoes, intact and decapitated, with dsRNA corresponding to three domains of the *MIR* resulted in clear and specific depletion of receptor transcript by 12 h pbm (Fig. 5*A*). Receptor protein was in turn reduced at 12 h pbm and depleted at 72 h when females begin laying eggs (Fig. 5*B*). We therefore asked whether *MIR* knockdown disables egg maturation by comparing yolk uptake and ecdysteroid production in intact blood-fed females pretreated with *dsMIR* versus control females pretreated with *dsGFP* or water. These experiments indicated that *dsMIR* treatment greatly reduced yolk uptake and ecdysteroid production compared with the controls, suggesting that endogenous ILPs failed to activate egg maturation in the absence of MIR expression (Fig. 5 *B* and *C*). *In vitro* assays that measured ecdysteroid production by the ovaries supported this interpretation by indicating that ILP3 activity also depends on MIR expression (Fig. 5*D*). Ovaries collected from females that had been decapitated and treated with water or *dsGFP* immediately pbm produced, as expected, only basal levels of ecdysteroids, but these ovaries readily

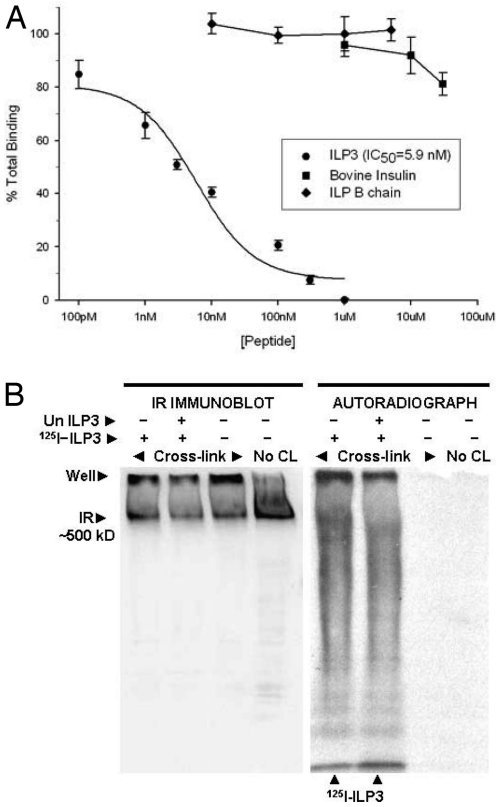

Fig. 4. ILP3 binds to ovary membranes. (*A*) Binding of ^{125}I-ILP3 to ovary membranes in the presence of increasing concentrations of unlabeled ILP3, ILP3 B chain, or bovine insulin. Bound counts in the presence of increasing concentrations of each unlabeled competitor, minus nonspecific binding, are plotted as a decreasing percentage of total binding (see *Materials and Methods*). IC_{50} value for ILP3 is presented in the enclosed box. (*B*) ^{125}I-ILP3 binds to a high molecular mass complex containing the MIR. Ovary membranes (50–60 ovary pair equivalents) were incubated with labeled (250 pmol) and unlabeled (2.5 μM) ILP3. After cross-linking, samples were analyzed by SDS/PAGE and immunoblotting. (*Left*) The immunoblot was probed with a β chain-specific MIR antibody (1:5,000). (*Right*) The autoradiograph visualizes ^{125}I-ILP3. Bound label localizes to a single band in the cross-linked sample; unbound label (arrows) is at the bottom of the gel.

produced ecdysteroids when ILP3 (20 pmol) was added to cultures (Fig. 5*D*). In contrast, ILP3 did not induce ovaries from decapitated females treated with *dsMIR* to produce significantly more ecdysteroids (Fig. 5*D*). Equivalent results were obtained with a higher amount of bovine insulin (1 nmol) (data not shown).

Discussion

Although bovine insulin stimulates ecdysteroid production by *A. aegypti* ovaries, the high concentration range required (14, 16) and its inability to stimulate yolk deposition by oocytes at any concentration (M.R.B. and M.R.S., unpublished observations) suggested mammalian insulins are weak agonists for the endogenous ILPs regulating these processes. That differences in ligand binding affinities may exist was further supported by sequence analysis that revealed considerable divergence between mosquito ILPs and insulin and the predicted ligand binding domains of the MIR and human IR. Our functional assays supported this conclusion by showing that ILP3 stimulates ecdysteroid production by ovaries and yolk uptake by oocytes at lower concentrations than bovine insulin. ILP3 also bound to ovary membranes with high affinity and was poorly competed by bovine insulin, whereas our RNAi data indicate the MIR is essential for ILP3 activity.

The response of mammalian tissues to insulin depends on both IR expression levels and signaling pathway interactions (29–31). Binding affinities for mammalian insulins vary from 0.1 to 1 nM with highly purified IR to IC_{50} ratios of 0.7–12.8 nM using membrane preparations from tissues expressing high levels of receptor (30, 33). The IC_{50} ratio determined for ILP3 (5.9 nM) using ovary membranes with high MIR expression (17) compares favorably with these values and with values for ILP1 from *B. mori* binding to an unknown receptor expressed by a lepidopteran cell line (34, 35). Our immunoblotting and autoradiography experiments strongly suggest ILP3 binds the MIR, but the molecular mass of the ILP3–MIR complex after cross-linking combined with the inability to fully displace ILP3 using cold competitor also raises questions about the nature of this interaction. One possibility is that ILP3 binding requires interaction between the MIR and other currently unknown proteins. Another is that ILP3 binding requires clustering of the MIR into a high molecular mass complex given the apparent absence of ILP3 binding to the homodimeric (500 kDa) form of the receptor.

Insulin binding to the IR is usually associated with the regulation of metabolic responses, whereas IGF binding to the IGFR is associated with longer-term mitogenic effects. More recent studies though indicate that insulin and IGFs can bind hybrid receptors of IR and IGFR monomers, resulting in greater activity spectra than previously assumed (29–32). In addition to their mitogenic activities, IGFs produced in the nervous system of mammals also regulate reproduction and steroid hormone secretion (36, 37), suggesting an interesting parallel with invertebrates given results of the current study. Less clear is whether mosquito and other insect ILPs have overlapping activities and how activity may be regulated when only one IR/IGFR homolog and fewer isoforms of downstream signaling components are present (8, 9). Genetic ablation of MNCs and the *Drosophila* IR (DIR) in *Drosophila* indicate that ILPs from the nervous system have metabolic and cell growth activity but do not reveal whether specific ILPs have differing biological activities (38–41). Genetic studies also show that the DIR predominantly stimulates the PI3K/AKT pathway although some data also suggest activation of the MAPK pathway (7). Our results strongly indicate that ILP3 has both egg development and metabolic activity but do not address whether other mosquito ILPs have these activities or MIR activation stimulates signaling through one or more pathways. Another unresolved issue is the role of ILP3 relative to ovary ecdysteroidogenic hormone (OEH) that also stimulates ecdysteroid production (13). The mode of action for OEH is unknown, but sequence similarity to IGF binding proteins (IGFBPs) intriguingly suggests ILPs and OEH may interact to activate the MIR in a manner similar to the interaction between IGFs and IGFBPs in activating IGFRs (42). That *Drosophila* (5) and *A. aegypti* (M.R.B. and M.R.S., unpublished results) encode relaxin GPCR homologs offers another potential candidate receptor for insect ILP family members. Although not explored in this study, mosquito ILPs may also coordinate metabolism in blood-fed females to replenish stores needed for other reproductive cycles (43). Given the importance of nutrient availability for pathogen development, this idea raises the possibility that insulin signaling plays a critical role in linking blood feeding, egg maturation, and pathogen transmission by mosquitoes to human and other mammalian hosts.

Materials and Methods

Mosquitoes. Experiments were conducted with the UGAL strain of *A. aegypti* (15).

Sequence Analysis and Structural Modeling. Sequence comparisons were made by using BLAST (www.ncbi.nlm.nih.gov/BLAST). Alignments were generated with Clustal W and DNAStar software. Homology models were constructed by using the Swiss Model (http://swissmodel.expasy.org//SWISS-MODEL.html). ILP sequences were threaded onto either the A or B chain of the T6 human insulin (Protein Data Bank ID code 1MSO) or human relaxin 2 (Protein Data Bank ID code

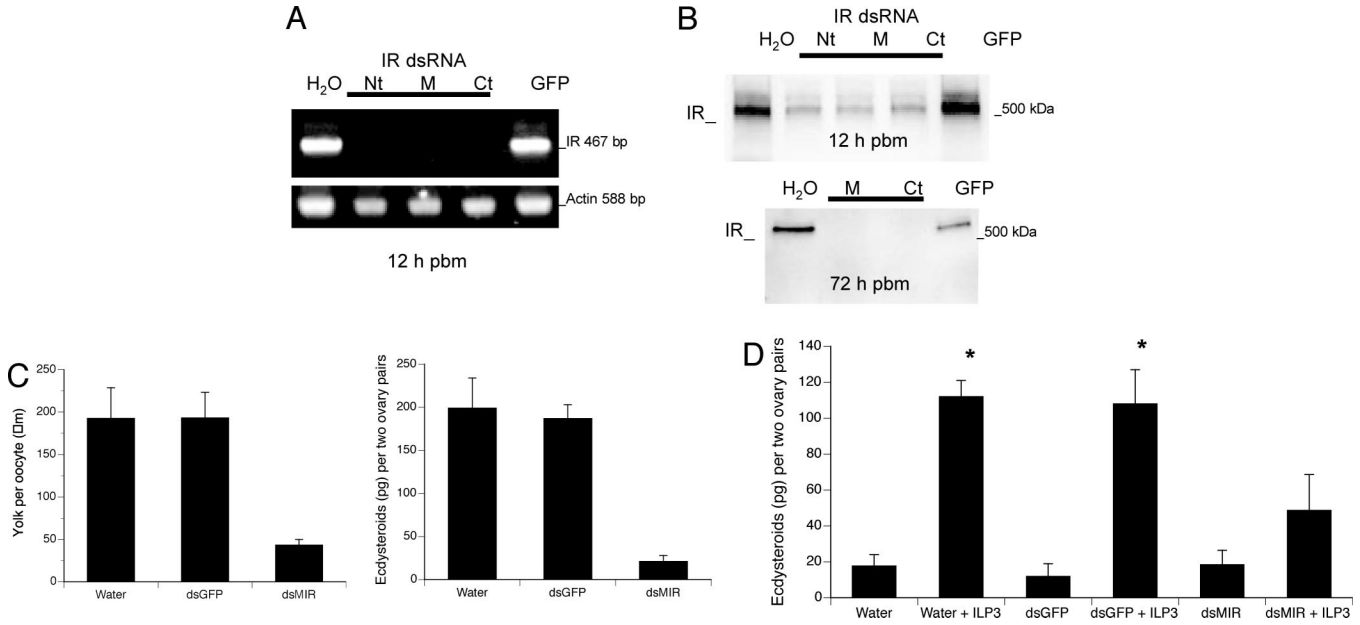

Fig. 5. *MIR* knockdown disables ILP activity. Female *A. aegypti* were treated with *dsMIR* corresponding to the N-terminal (Nt), Middle (M), and C-terminal (Ct) domains of the MIR ORF. Controls were mosquitoes treated with water or *GFP dsRNA*. (*A*) RT-PCR of *MIR* in ovaries from mosquitoes treated 12 h earlier with *dsMIR*, water, or *dsGFP*. Amplification of actin from the same sample served as the control. (*B*) Immunoblot of ovary proteins (one ovary pair equivalent per lane) isolated from mosquitoes 12 and 72 h after treatment with *dsMIR*, water, or *dsGFP* probed with anti-MIR (1:5k). (*C*) *MIR* knockdown inhibits yolk uptake by oocytes (*Left*) and ecdysteroid synthesis by ovaries (*Right*) in blood-fed females. Yolk per oocyte ($F_{2,\ 108} = 135.8$; $P < 0.001$) and ecdysteroids per two ovary pairs ($F_{2,21} = 31.7$; $P < 0.001$) were significantly less in mosquitoes treated with *dsMIR* than in mosquitoes treated with water or *dsGFP*. (*D*) *MIR* knockdown reduces ecdysteroid synthesis by ovaries incubated with ILP3 *in vitro*. Females were decapitated after pbm and injected with *dsMIR*, water, or *dsGFP*. Ovaries were then dissected from females 24 h later with ecdysteroid production measured for two ovary pairs incubated with or without ILP3 (20 pmol). Asterisks indicate treatments that differed significantly from the negative control (water) ($F_{5,36} = 27.3$; $P < 0.001$). Results from females treated with the three *dsMIR* domains were pooled for analysis in *C* and *D*.

6RLX) crystal structures in the DeepView program by using the Magic Fit application to generate preliminary models and alignments. Models were then submitted to the Swiss-Model comparative server (http://swissmodel.expasy.org) (44). Resulting structures were automatically regularized in the last modeling step by steepest descent energy minimization using the GROMOS96 force field. Models were then analyzed by atomic mean force potential (ANOLEA), GROMOS, and Verify 3D (45).

ILP3 Synthesis. The A and B chains of ILP3 were synthesized on an Applied Biosystems 433 synthesizer using standard Fmoc chemistry. Each peptide resin was cleaved and deprotected in reagent K (46). Peptides were then precipitated and washed in cold *t*-butylmethyl ether and air-dried. Formation of the correct intrachain and interchain disulfide bonds between the A and B chains followed previous work (25). Briefly, the A chain was synthesized with Cys(Trt) groups at positions 6 and 11, Cys(acm) at position 7, and Cys(tBu) at position 20. The B chain contained Met-sulfoxide at position 16, a Cys(acm) at position 6, and a Cys(Trt) at position 18. Trt groups were removed during deprotection, leaving the acm and tBu protecting groups intact. At each step of the subsequent synthesis, products were purified by HPLC and identified by MALDI-TOF MS. To form the internal disulfide of the A chain, the two free thiols at positions 6 and 11 were oxidized by I_2 treatment in AcOH. To combine the two chains, the A chain was activated by removing the tBu-protecting group [using trifluoroacetic acid (TFA), thioanisole, and trifluoromethanesulfonic acid] and replacing it with SPyr (using dipyridyldisulfide), a protecting group subject to attack by the free thiol (Cys^{18}) of the B chain (24). The activated A chain and B chain were combined at a 1:1.5 ratio with the reaction completed by 1.5 h. The last disulfide was formed by I_2-induced removal of the acm-protecting groups at Cys^7 (A chain) and Cys^6 (B chain) and concomitant oxidation of the thiols. Finally, the Met-sulfoxide was reduced by NH_4I and DMS (47). After purification, ILP3 was lyophilized, rehydrated in water, and frozen (−80°C) for use in bioassays.

Immunocytochemistry and Blotting. Brains were processed for ILP localization by using a mAb to BmILPA1 (15). For dot blots, Bm-ILPA1, bovine insulin (Sigma), and AaILP3 were spotted onto nitrocellulose, incubated with anti-BmILPA1 (1: 4,000) overnight, and detected by using goat anti-rabbit IgG horseradish peroxidase (Sigma) and chemiluminescence (Amersham ECL) using a GeneGnome (SynGene) imager.

Bioassays. For the *in vivo* egg maturation assay, blood-fed females were decapitated within 1 h pbm, injected with graded amounts of ILP3 in 0.5 μl of saline, and examined for yolk protein deposition in oocytes 24 h later (13). Decapitated females injected with saline served as negative controls and intact blood-fed females served as positive controls. For the *in vitro* assay of ovarian ecdysteroid production, triplicate sets of ovaries (two or four pairs/60 μl in a polypropylene cap) from nonblood-fed females were incubated alone (control) or with serially diluted doses of ILP3 in media for 6 h at 27°C. Ecdysteroids in media (50 μl per cap) were quantified by RIA (48). Results were reported for one to three experiments (each with three ovary sets per dose) using different female cohorts. For metabolic assays, starved females (water only for up to 6 days posteclosion) were given a 10% sucrose solution for 30 min, and only those with swollen abdomens were either left intact for controls or decapitated and injected with saline (control) or ILP3 (6–8 females per dose; total injected volume of 0.5 μl per female). After 6 and 24 h at 27°C, females were separated into samples of two per tube, whereupon 100 μl of saturated Na_2SO_4 was added, and the samples were frozen (−80°C). Whole body homogenates were partitioned and assayed for total soluble carbohydrates, glycogen, and lipid (triglyceride) as described (49). Each metabolite was measured in triplicate by using different cohorts with results reported in micrograms of metabolite per female.

Receptor Binding and Cross-Linking Assays. ILP3 was iodinated by using the lactoperoxidase–hydrogen peroxide method and purified by HPLC (50). Fractions containing ^{125}I-ILP3 (fraction V BSA added to 1%) were diluted and counted to determine final concentration (≈25–27 nM) based on specific activity (≈2,000 Ci/mmol) of ^{125}I in the product free of unlabeled peptide. Ovary membranes were prepared from 500 ovary pairs (4-day-old nonblood-fed females) in buffer [50 mM Tris·HCl (pH 7.5), 250 mM sucrose, 2× protease inhibitor (PI), Roche complete mini protease inhibitor tablet], pooled into one 1.5-ml microtube by brief centrifugation (13,000 × *g*, 1 min. 4°C), homogenized with a pestle (2 × 30 s), and sonicated, while iced. After centrifugation (2,000 × *g*, 5 min at 4°C), the supernatant solution was transferred to a 1.5-ml microtube for centrifugation (48,000 × *g*, 1 h at 4°C). The supernatant solution was discarded, and the ovary

membrane pellet was dispersed with a pestle in 800 μl of binding buffer [1× Hank's balanced salt solution (10X stock; GIBCO/BRL), 50 mM Hepes (pH. 7.6), 1% BSA, and 1× PI] before storage at −80°C.

Binding experiments were in triplicate for each treatment using ice-chilled solutions. To each 1.5-ml microtube, 30 μl of unlabeled ILP3 at 10× concentration of the desired final concentration (0.1 nM to 1 μM) was added to 100 μl of binding buffer containing ≈100–200 pmol of ^{125}I-ILP3 (≈200,000 to 300,000 cpm), followed by 70 μl of the membrane solution (≈20 ovary pairs) and then 100 μl of binding buffer (total 300 μl). After a brief vortex, the tubes were rotated overnight at 4°C, and then centrifuged at 20,000 × *g* for 5 min at 4°C. Supernatants were aspirated from the pelleted membranes, which were then rinsed with 300 μl of ice-cold binding buffer, centrifuged, and aspirated again. Raw counts obtained from the pellets were converted to percent total binding, and these data were analyzed by nonlinear regression analysis with Sigma Plot software to obtain curves, IC_{50} values (the concentration of ILP3 that reduces specific binding of ^{125}I-ILP3 by 50%), and statistics, including values of R^2 and standard errors. For cross-linking, ovary membranes were prepared as above (50–75 ovary pair equivalents per tube) and incubated overnight (4°C) alone or with 200–300 pmol of ^{125}I-ILP3 in the presence or absence of 1–5 μM unlabeled ILP3 (300 μl total volume). Subsequently, the cross-linking agent, *Bis*[sulfosuccin-imidyl] suberate, in water was added to 200 μM, and the membranes were rotated for 1 h at 4°C. Reactions were stopped with ≈100 mM Tris buffer (pH 7.5), and pelleted membranes were frozen in water. Membranes were then mixed with sample buffer (nonreducing), sonicated, denatured (90°C, 10 min), and loaded onto a Tris·HCL 4–20% gel (BioRad Criterion) for electrophoresis and blotting onto nitrocellulose (Protran 0.2 μm; Schleicher & Schuell) (17). Blots were incubated sequentially with affinity-purified antibody to the C-terminal region of the MIR (1: 5,000 of antibody 377) and goat anti-rabbit IgG–horseradish peroxidase (Sigma; 1: 40,000). Immunolabeled MIR was then visualized by chemiluminescence as described above, and ILP3 was visualized by autoradiography using Kodak XR film.

RNAi Assays. MIR cDNA was amplified with forward and reverse primers with the T7 sequence at their 5′ ends corresponding to the amino terminus (Nt-; nucleotides 250–732), middle (M-; nucleotides 2173–2647), and carboxyl terminus (Ct-; nucleotides 3079–3546), where no other homology was found by BLAST search (National Center for Biotechnology Information). Purified PCR products (Qiaprep; Qiagen) were used as templates for dsRNA synthesis with the MEGAscript T7 kit (Ambion). Briefly, 1 μg of template cDNA was transcribed *in vitro* by using T7 polymerase. dsRNA was then treated with DNase1 and RNase1, precipitated, and resuspended in nanopure water. GFP dsRNA was generated as a control. Integrity of dsRNAs was assessed after gel electrophoresis, and concentration was determined by spectrophotometry for dilution to 4 μg/μl before storage at −20°C. dsRNAs in 0.5 μl of water were injected into intact or decapitated females (3 to 5 days old) at 1 h pbm followed by reproduction bioassays as described above. Ovaries were processed for RT-PCR and immunoblotting as described above to assess MIR expression.

ACKNOWLEDGMENTS. We thank Dr. E. Büllesbach (Medical University of South Carolina, Charleston, SC) for BmILPA1 and Dr. A. Mizoguchi (Nagoya University, Nagoya, Japan) for anti-BmILPA1. This work was supported by National Institutes of Health Grant AI03108 and the Georgia Agricultural Experiment Station.

1. Murray-Rust J, McLeod AN, Blundell TL (1992) Structure and evolution of insulins: Implications for receptor binding. *BioEssays* 14:325–331.
2. De Meyts P (2004) Insulin and its receptor: Structure, function, and evolution. *BioEssays* 26:1351–1362.
3. Pierce SB, *et al.* (2001) Regulation of DAF-2 receptor signaling by human insulin and ins-1, a member of the unusually large and diverse *C. elegans* insulin gene family. *Genes Dev* 15:672–686.
4. McDonald N, Murray-Rust J, Blundell T (1989) Structure–function relationships of growth factors and their receptors. *Br Med Bull* 45:554–569.
5. Halls ML, van der Westhuizen ET, Bathgate RAD, Summers RJ (2007) Relaxin family peptide receptors: Former orphans reunite with their parent ligands to activate multiple signalling pathways. *Br J Pharmacol* 150:677–691.
6. Liu C, *et al.* (2005) INSL5 is a high affinity-specific agonist for GPCR142-GPR100. *J Biol Chem* 280:292–300.
7. Brogiolo W, *et al.* (2001) An evolutionarily conserved function of the *Drosophila* insulin receptor and insulin-like peptides in growth control. *Curr Biol* 11:213–221.
8. Wu Q, Brown MR (2006) Signaling and function of insulin-like peptides in insects. *Annu Rev Entomol* 51:1–24.
9. Leevers SJ (2001) Growth control: Invertebrate insulin surprises! *Curr Biol* 11:R209–R212.
10. Attardo GM, Hansen IA, Raikhel AS (2005) Nutritional regulation of vitellogenesis in mosquitoes: Implications for anautogeny. *Insect Biochem Mol Biol* 35:661–675.
11. Lea AO (1967) The medial neurosecretory cells and egg maturation in mosquitoes. *J Insect Physiol* 13:419–429.
12. Matsumoto S, Brown MR, Suzuki A, Lea AO (1989) Isolation and characterization of ovarian ecdysteroidogenic hormones from the mosquito, *Aedes aegypti*. *Insect Biochem* 19:651–656.
13. Brown MR, *et al.* (1998) Identification of a steroidogenic neurohormone in female mosquitoes. *J Biol Chem* 273:3967–3971.
14. Riehle MA, Brown MR (1999) Insulin stimulates ecdysteroid production through a conserved signaling cascade in the mosquito *Aedes aegypti*. *Insect Biochem Mol Biol* 29:855–860.
15. Riehle MA, Fan Y, Cao C, Brown MR (2006) Molecular characterization of insulin-like peptides in the yellow fever mosquito, *Aedes aegypti*: Expression, cellular localization, and phylogeny. *Peptides* 27:2535–3028.
16. Graf R, Neuenschwander S, Brown MR, Ackermann U (1997) Insulin-mediated secretion of ecdysteroids from mosquito ovaries and molecular cloning of the insulin receptor homologue from ovaries of blood-fed *Aedes aegypti*. *Insect Mol Biol* 6:151–163.
17. Riehle MA, Brown MR (2002) Insulin receptor expression during development and a reproductive cycle in the ovary of the mosquito *Aedes aegypti*. *Cell Tissue Res* 308:409–420.
18. Riehle MA, Brown MR (2003) Molecular analysis of the serine/threonine kinase Akt and its expression in the mosquito *Aedes aegypti*. *Insect Mol Biol* 12:225–232.
19. Wilkinson TN, Speed TP, Tregear GW, Bathgate RA (2005) Evolution of the relaxin-like peptide family. *BMC Evol Biol* 5:14.
20. Mirmira RG, Nakagawa SH, Tager HS (1991) Importance of the character and configuration of residues B24, B25, and B26 in insulin-receptor interactions. *J Biol Chem* 266:1428–1436.
21. Huang K, *et al.* (2004) How insulin binds: The B-chain α-helix contacts the L1 β-helix of the insulin receptor. *J Mol Biol* 341:529–550.
22. Xu B, *et al.* (2004) Diabetes-associated mutations in insulin identify invariant receptor contacts. *Diabetes* 53:1599–1602.
23. Goeddel DW, *et al.* (1979) Expression in *Escherichia coli* of chemically synthesized genes for human insulin. *Proc Natl Acad Sci USA* 76:106–110.
24. Maruyama K, *et al.* (1992) Synthesis of bombyxin-IV, an insulin superfamily peptide from the silkworm, *Bombyx mori*, by stepwise and selective formation of three disulfide bridges. *J Protein Chem* 11:1–12.
25. Büllesbach EE, Schwabe C (2006) The mode of interaction of the relaxin-like factor (RLF) with the leucine-rich repeat G protein-activated receptor 8. *J Biol Chem* 281:26136–26143.
26. Meola SM, Lea AO (1972) The ultrastructure of the corpus cardiacum of *Aedes sollicitans* and the histology of the cerebral neurosecretory system of mosquitoes. *Gen Comp Endocrinol* 18:210–234.
27. Kahn SE, Hull RL, Utzschneider KM (2006) Mechanisms linking obesity to insulin resistance and type 2 diabetes. *Nature* 444:840–846.
28. Kristensen C, Wiberg FC, Schaffer L, Andersen AS (1998) Expression and characterization of a 70-kDa fragment of the insulin receptor that binds insulin: Minimizing ligand binding domain of the insulin receptor. *J Biol Chem* 273:17780–17786.
29. Blakesley VA, Scrimgeour A, Esposito D, Le Roith D (1996) Signaling via the insulin-like growth factor-I receptor: Does it differ from insulin receptor signaling? *Cytokine Growth Factor Rev* 7:153–159.
30. Siddle K, *et al.* (2001) Specificity in ligand binding and intracellular signaling by insulin and insulin-like growth factor receptors. *Biochem Soc Trans* 29:513–525.
31. Pandini G, *et al.* (2002) Insulin/insulin-like growth factor I hybrid receptors have different biological characteristics depending on the insulin receptor isoform involved. *J Biol Chem* 277:39684–39695.
32. Taniguchi CM, Emanuelli B, Kahn CR (2006) Critical nodes in signaling pathways: Insights into insulin action. *Nat Rev Mol Cell Biol* 7:85–96.
33. Joost HG (1995) Structural and functional heterogeneity of insulin receptors. *Cell Signal* 7:85–91.
34. Tanaka M, Kataoka H, Nagata K, Nagasawa H, Suzuki A (1995) Morphological changes of BM-N4 cells induced by bombyxin, an insulin-related peptide of *Bombyx mori*. *Regul Pept* 57:311–318.
35. Fullbright G, Lacy ER, Bullesbach EE (1997) The prothoracicotropic hormone bombyxin has specific receptors on insect ovarian cells. *Eur J Biochem* 245:774–780.
36. Richards JS, *et al.* (2002) Novel signaling pathways that control ovarian follicular development, ovulation, and luteinization. *Rec Prog Horm Res* 57:195–220.
37. Daftary SS, Gore AC (2005) IGF-1 in the brain as a regulator of reproductive neuroendocrine function. *Exp Biol Med* 230:292–306.
38. Ikeya T, Galic M, Belawat P, Nairz K, Hafen E (2002) Nutrient-dependent expression of insulin-like peptides from neuroendocrine cells in the CNS contributes to growth regulation in *Drosophila*. *Curr Biol* 12:1293–1300.
39. Rulifson EJ, Kim SK, Nusse R (2002) Ablation of insulin-producing neurons in flies: Growth and diabetic phenotypes. *Science* 296:1118–1120.
40. Broughton SJ, *et al.* (2005) Longer lifespan, altered metabolism, and stress resistance in *Drosophila* from ablation of cells making insulin-like ligands. *Proc Natl Acad Sci USA* 102:3105–3110.
41. Belgacem YH, Martin JR (2006) Disruption of insulin pathways alters trehalose level and abolishes sexual dimorphism in locomotor activity in *Drosophila*. *J Neurobiol* 66:19–32.
42. Claeys I, Simonet G, Van Loy T, De Loof A, Vanden Broeck J (2003) cDNA cloning and transcript distribution of two novel members of the neuroparsin family in the desert locust, *Schistocerca gregaria*. *Insect Mol Biol* 12:473–481.
43. Roy SG, Hansen IA, Raikhel AS (2007) Effect of insulin and 20-hydroxyecdysone in the fat body of the yellow fever mosquito, *Aedes aegypti*. *Insect Biochem Mol Biol* 37:985–997.
44. Schwede T, Kopp J, Guex N, Peitsch MC (2003) SWISS-MODEL: An automated protein homology-modeling server. *Nucleic Acids Res* 31:3381–3385.
45. van Gunsteren WF, *et al.* (1996) *Biomolecular Simulations: The GROMOS96 Manual and Users Guide* (VdF Hochschulverlag Eidgenössische Technische Hochschule, Zurich).
46. King DS, Fields CG, Fields GB (1990) A cleavage method which minimizes side reactions following Fmoc solid-phase peptide synthesis. *Int J Pept Res* 36:255–266.
47. Vilaseca M, Nicolas E, Capdevila F, Giralt E (1998) Reduction of methionine sulfoxide with NH_4I/TFA: Compatibility with peptides containing cysteine and aromatic amino acids. *Tetrahedron* 54:15273–15286.
48. Sieglaff DH, Duncan KA, Brown MR (2005) Expression of genes encoding proteins involved in ecdysteroidogenesis in the female mosquito, *Aedes aegypti*. *Insect Biochem Mol Biol* 35:369–514.
49. Telang A, Wells MA (2004) The effect of larval and adult nutrition on successful autogenous egg production by a mosquito. *J Insect Physiol* 50:677–676.
50. Crim JW, Garczynski SF, Brown MR (2002) Approaches to radioiodination of insect peptides. *Peptides* 23:2045–2051.